Thermochimica Acta 478 (2008) 13–16

Contents lists available at ScienceDirect

Thermochimica Acta

journal homepage: www.elsevier.com/locate/tca

Heat capacity of $Sr_{10}(PO_4)_6Cl_2$ and $Ca_{10}(PO_4)_6Cl_2$ by DSC

R. Venkata Krishnan[a], Hrudananda Jena[b], K.V. Govindan Kutty[b], K. Nagarajan[a,*]

[a] Fuel Chemistry Division, Indira Gandhi Centre for Atomic Research, Kalpakkam 603102, India
[b] Liquid Metals and Structural Chemistry Division, Indira Gandhi Centre for Atomic Research, Kalpakkam 603102, India

ARTICLE INFO

Article history:
Received 21 May 2008
Received in revised form 12 August 2008
Accepted 20 August 2008
Available online 28 August 2008

Keywords:
Heat capacity
Chloroapatites
Radioactive waste immobilization
Apatites
DSC

ABSTRACT

Strontium and calcium chloroapatites were synthesized by wet chemical method, characterized by X-ray diffraction and are found to be phase pure materials. The measured room temperature lattice parameter of $Ca_{10}(PO_4)_6Cl_2$ is $a = 9.523$ Å, $c = 6.855$ Å and for $Sr_{10}(PO_4)_6Cl_2$ is $a = 9.876$ Å, $c = 7.188$ Å. Heat capacity measurements were carried out on $Ca_{10}(PO_4)_6Cl_2$ and $Sr_{10}(PO_4)_6Cl_2$ by DSC in the temperature range 298–800 K. The heat capacity values of $Sr_{10}(PO_4)_6Cl_2$ is higher at all temperatures than $Ca_{10}(PO_4)_6Cl_2$. Enthalpy and entropy increments were computed. Heat capacity values of $Ca_{10}(PO_4)_6Cl_2$ and $Sr_{10}(PO_4)_6Cl_2$ at 298 K are 758 and 868 J K^{-1} mol^{-1}, respectively.

1. Introduction

Several studies are conducted worldwide to find new host forms for immobilizing radioactive wastes [1–9]. The candidature of a material for radioactive waste immobilization is decided based on its properties such as resistance to thermal degration, ability to accommodate significant quantities of radioactive nuclides in their structure, cost effectiveness, etc. [3]. Apatites are considered to be among suitable solid host matrices for immobilizing chloride wastes generated by pyrochemical reprocessing of spent fuel. Apatites are naturally occurring minerals having hexagonal crystal structure ($P6_3/m$ space group) with a unit cell formula of $M_5(PO_4)_3(X)$, M = Ca, Sr, Ba, and (X = OH, Cl or F) [10,11]. These apatites can immobilize highly active and heat generating radioactive elements such as ^{90}Sr, ^{137}Cs, ^{99}Tc, etc. and halide ions [12] by accommodating them in their crystal lattice by forming substitutional solid solution [13]. The attractive feature of the apatites for nuclear waste immobilization is their ease of preparation at low temperature. Thermodynamic data such as heat capacity, thermal conductivity, etc. of the chloroapatites are essential to understand their phase behavior after immobilizing the chloride, alkali and alkaline earth fission products into the apatite structure. There are no measured heat capacity data for these compounds. Therefore, in the present study, heat capacity measurements were carried out on the phase pure $Ca_{10}(PO_4)_6Cl_2$ and $Sr_{10}(PO_4)_6Cl_2$ by DSC and the experimental results are discussed in this paper.

2. Experimental

2.1. Synthesis and characterization

$SrCl_2$, $CaCl_2$ and $NH_4H_2PO_4$ of 99.99% purity supplied by M/s. SD-Fine Chemicals, India were used for the preparation of the samples. Stiochiometric quantities of $SrCl_2$, $CaCl_2$ and $NH_4H_2PO_4$ were dissolved in deionized water, and mixed and stirred. The pH of the mixture was maintained in the range of 9–10, by addition of aqueous ammonia. The white precipitate formed was filtered, washed with deionized water and oven dried. The dried powders of $Ca_{10}(PO_4)_6Cl_2$ and $Sr_{10}(PO_4)_6Cl_2$ formed were characterized by X-ray powder diffraction, employing a Siemens D-500 powder X-ray diffractometer in the step scan mode using Cu Kα radiation. Purity of the samples were estimated by using ICP-MS. The total impurities in both $Ca_{10}(PO_4)_6Cl_2$ and $Sr_{10}(PO_4)_6Cl_2$ are less than 0.1 mol.%. $Ca_{10}(PO_4)_6Cl_2$ and $Sr_{10}(PO_4)_6Cl_2$ powders were then compacted into pellets of 5 mm in diameter and sintered by heating at 1273 K for 10 h in air. The sintered pellets were used for heat capacity measurements.

2.2. Heat capacity measurements

A heat flux type differential scanning calorimeter (model number DSC821e/700 of M/s. Mettler Toledo GmbH, Switzerland) was

---

[*] Corresponding author at: Fuel Chemistry Division, Indira Gandhi Centre for Atomic Research, Chemistry Group, Kalpakkam 603102, India.
Tel.: +91 44 27480500x24289; fax: +91 44 27480065.
E-mail address: knag@igcar.gov.in (K. Nagarajan).

0040-6031/$ – see front matter © 2008 Elsevier B.V. All rights reserved.
doi:10.1016/j.tca.2008.08.009

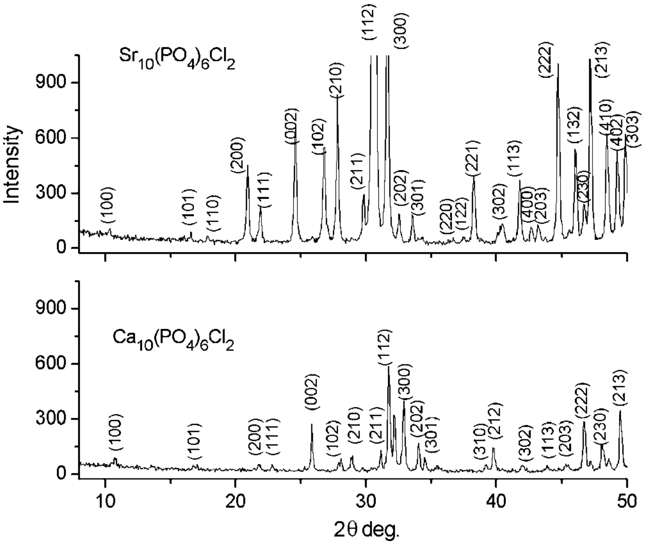

Fig. 1. XRD pattern of $Ca_{10}(PO_4)_6Cl_2$ and $Sr_{10}(PO_4)_6Cl_2$.

Table 2
Experimental heat capacity data of $Ca_{10}(PO_4)_6Cl_2$ and $Sr_{10}(PO_4)_6Cl_2$

T (K)	$C_{p,m}$ (J K^{-1} mol^{-1})	
	$Ca_{10}(PO_4)_6Cl_2$	$Sr_{10}(PO_4)_6Cl_2$
298	758	868
300	769	870
320	788	896
340	819	919
360	847	941
380	871	960
400	892	980
420	913	1000
440	933	1019
460	950	1035
480	965	1054
500	983	1071
520	1000	1085
540	1015	1095
560	1031	1109
580	1039	1118
600	1050	1128
620	1062	1138
640	1074	1143
660	1082	1142
680	1090	1147
700	1099	1152
720	1101	1153
740	1107	1148
760	1108	1157
780	1106	1151
800	1103	1150

used in this study. The sintered pellet samples were hermetically sealed in 40 µl Al-pans. High purity argon was used as the purge gas at a flow rate of 50 ml min^{-1} and a heating rate of 10 K min^{-1} was employed in DSC measurements in the temperature range 298–800 K. A thin disc of sapphire was used as the heat capacity standard. A three segment-heating programme was used. The first segment lasting for 5 min was an isothermal one at the initial temperature; the second segment was a dynamic one with a heating rate of 10 K min^{-1} and the final segment lasting for 5 min was another isothermal one at the final temperature. Temperature, heat and heat rate calibrations of the DSC were carried out as it was explained in our earlier work [14].

3. Results and discussion

The phase purity of $Sr_{10}(PO_4)_6Cl_2$ and $Ca_{10}(PO_4)_6Cl_2$ compositions were confirmed by XRD examination of the powders as shown in Fig. 1. However, when the samples were pelletized and heated at 1273 K for 10 h and the XRD were taken, the pattern showed minor peaks (peak intensity <1%) corresponding to $Sr_3(PO_4)_2$ and $Ca_3(PO_4)_2$. This may be due to the loss of chloride from the surface of the pellets, when heated at high temperature. When these pellets were broken, ground using mortar and pestle, the XRD-pattern of these powders did not indicate any additional minor peaks of $Sr_3(PO_4)_2$ and $Ca_3(PO_4)_2$. The compositions were indexed to hexagonal unit cell (SG = $P6_3/m$) by using X'pert pro software. The lattice parameters of $Ca_{10}(PO_4)_6Cl_2$ and $Sr_{10}(PO_4)_6Cl_2$ determined in the present study are listed in Table 1. As can be seen from Table 1, the present lattice parameter data are in good agreement with the values reported in the literature [15–17]. The lattice parameter of $Sr_{10}(PO_4)_6Cl_2$ is higher than that of $Ca_{10}(PO_4)_6Cl_2$ due to the larger ionic radius of Sr^{2+} ($r^{VIII}_{Sr^{2+}} = 1.40$ Å, $r^{IX}_{Sr^{2+}} = 1.45$ Å) compared to Ca^{2+} ($r^{VIII}_{Ca^{2+}} = 1.26$ Å, $r^{IX}_{Ca^{2+}} = 1.32$ Å) [18].

Heat capacity data of sapphire given by National Institute of Standards and Technology, USA (NIST) were used for computing the heat capacities of the samples. Heat capacity of $Ca_{10}(PO_4)_6Cl_2$ and $Sr_{10}(PO_4)_6Cl_2$ measured by DSC and given in Table 2 are the mean of eight measurements. The relative standard deviations are in the range of 1–2%. The measured heat capacity data of $Ca_{10}(PO_4)_6Cl_2$ and $Sr_{10}(PO_4)_6Cl_2$ were least squares fitted to obtain the following polynomial in temperature:

$$C_{p,m}(Ca_{10}(PO_4)_6Cl_2)(\mathrm{J\,K^{-1}\ mol^{-1}}) = 276.43 + 2.0799\left(\frac{T}{K}\right) - 1.759390\times10^{6}\left(\frac{K}{T}\right)^{2} - 1.3\times10^{-3}\left(\frac{T}{K}\right)^{2}(298-800\ \mathrm{K}) \quad (1)$$

$$C_{p,m}(Sr_{10}(PO_4)_6Cl_2)(\mathrm{J\,K^{-1}\ mol^{-1}}) = 1138.26 + 0.09558\left(\frac{T}{K}\right) + 2.9031243\times10^{7}\left(\frac{K}{T}\right)^{2}(298-800\,\mathrm{K}) \quad (2)$$

Table 1
Crystal data for $Ca_{10}(PO_4)_6Cl2$ and $Sr_{10}(PO_4)_6Cl_2$ measured by XRD

Lattice parameters	Compound (space group $P6_3/m$ (176))			
	$Ca_{10}(PO_4)_6Cl_2$		$Sr_{10}(PO_4)_6Cl_2$	
	This study	Literature [9]	This study	Literature [10,11]
a (Å)	9.523 (3)	9.520	9.876 (4)	9.877
c (Å)	6.855 (3)	6.850	7.188 (3)	7.189
$\alpha = \beta$ (°)	90	90	90	90
Y (°)	120	120	120	120
Density (g/cm^3)	3.211 (1)		4.147 (2)	

Table 3
Thermodynamic functions of $Ca_{10}(PO_4)_6Cl_2$

T (K)	$C_{p,m}$ (J K^{-1} mol^{-1})		$H_T^0 - H_{298}^0$ (J mol^{-1})	S_T^0 (J K^{-1} mol^{-1})	$G_T^0 - H_{298}^0/T$ (J K^{-1} mol^{-1})
	Measured	Fit			
298	758	761	0	808	−808
300	769	764	1,527	813	−808
400	892	889	84,591	1051	−839
500	983	984	178,722	1260	−902
600	1050	1052	281,045	1446	−977
700	1099	1092	388,855	1611	−1056
800	1103	1106	499,510	1758	−1134

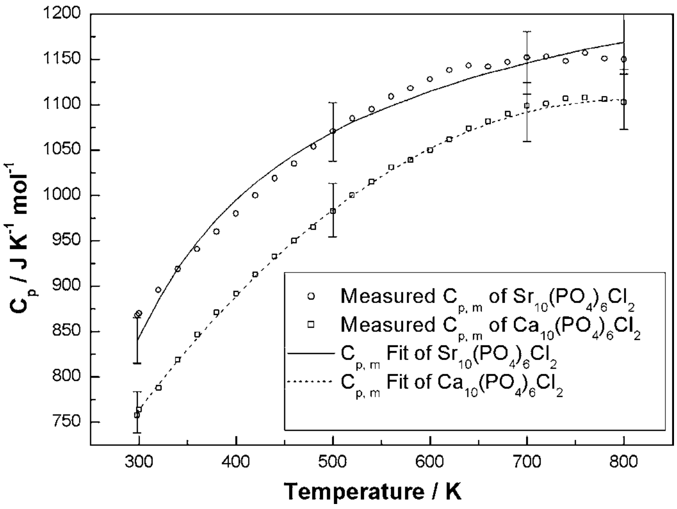

Fig. 2. Measured Cp values of $Ca_{10}(PO_4)_6Cl_2$ and $Sr_{10}(PO_4)_6Cl_2$.

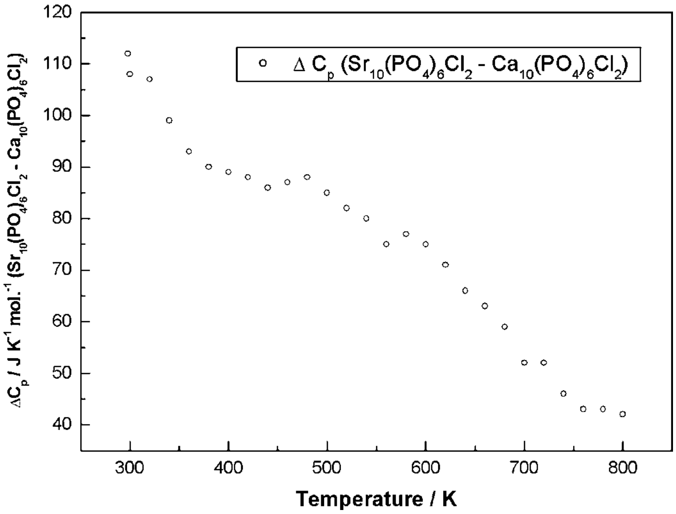

Fig. 3. Difference in heat capacity values between $Ca_{10}(PO_4)_6Cl_2$ and $Sr_{10}(PO_4)_6Cl_2$.

The standard errors of the fit for Eqs. (1) and (2) are 2.9 and 10.7 J K^{-1} mol^{-1}, respectively. The measured heat capacity data of $Ca_{10}(PO_4)_6Cl_2$ and $Sr_{10}(PO_4)_6Cl_2$ along with the fit values are shown in Fig. 2. From the heat capacity data, other thermodynamic functions such as enthalpy, entropy and Gibbs energy functions were computed for $Ca_{10}(PO_4)_6Cl_2$ and are given in Table 3. The S_{298}^0 value of $Ca_{10}(PO_4)_6Cl_2$ required for the computation of entropies was estimated by using Neumann–Kopp's additive rule from the literature data [19] of $Ca_3P_2O_8$ (235.98 J K^{-1} mol^{-1})[13] and $CaCl_2$ (105 J K^{-1} mol^{-1}) [19] besides including the contribution of ideal entropy of mixing. As there are no S_{298}^0 value available in the literature for $Sr_3P_2O_8$, only enthalpy and entropy increments were computed for $Sr_{10}(PO_4)_6Cl_2$ and are given in Table 4.

As seen in Fig. 2, the heat capacity data of $Sr_{10}(PO_4)_6Cl_2$ are higher than that of $Ca_{10}(PO_4)_6Cl_2$ at all temperatures. This is because of the well-known fact that the cationic contribution to the heat capacity increases with increase in atomic number in the same homologous series [20]. This is because higher the atomic mass of the element, lower will be the phonon frequencies and hence higher will be the heat capacity. But as the temperature is increased, the vibrational energy levels become more closely spaced due to anharmonicity and therefore the differences between the heat capacity of $Ca_{10}(PO_4)_6Cl_2$ and $Sr_{10}(PO_4)_6Cl_2$ decreases with increase in temperature as seen in Fig. 3.

Table 4
Thermodynamic functions of $Sr_{10}(PO_4)_6Cl_2$

T (K)	$C_{p,m}$ (J K^{-1} mol^{-1})		$H_T^0 - H_{298}^0$ (J mol^{-1})	$S_T^0 - S_{298}^0$ (J K^{-1} mol^{-1})
	Measured	Fit		
298	868	840	0	0
300	870	844	1,685	6
400	980	995	94,671	272
500	1071	1070	198,292	503
600	1128	1115	307,710	702
700	1152	1146	420,851	877
800	1150	1169	536,678	1031

4. Summary

Heat capacity measurements were carried out on $Ca_{10}(PO_4)_6Cl_2$ and $Sr_{10}(PO_4)_6Cl_2$ using DSC in the temperature range 298–800 K. The present data are the first ones for the heat capacity of above compounds. The difference between the heat capacity of $Sr_{10}(PO_4)_6Cl_2$ and $Ca_{10}(PO_4)_6Cl_2$ are larger at lower temperature and lower at high temperature.

References

[1] B.E. Burakov, Development of Fluorapatite as a Waste Form—Final Report, V.G. Khlopin Radium Institute, Saint-Petersburg, Russia, 2004.
[2] M. Hidouri, K. Bouzouita, F. Kooli, I. Khattech, Mater. Chem. Phys. 80 (2003) 496–505.
[3] J. Shi, K. Arndt, M. Shang, U. Bismayer, Am. Mineral. 88 (2003) 1866–1871.
[4] W. Lutze, R.C. Ewing (Eds.), Radioactive Waste Forms for the Future, Elsevier Science Publishing Company, Inc., Amsterdam, North Holland, 1988.
[5] R.C. Ewing, Proc. Natl. Acad. Sci. U.S.A. 96 (1999) 3432–3439.
[6] R.C. Ewing, Can. Mineral. 39 (3) (2001) 697–715.
[7] R.C. Ewing, W.J. Webber, F.W. Clinard, Prog. Nucl. Energ. 29 (2) (1995) 63–127.
[8] W.J. Webber, R.P. Turcotte, L.R. Bunnell, F.P. Roberts, J.H. Westsik, Radiation effects invitreous and devitrified simulated waste glass, in: T.D. Chikalla, J.E. Mendel (Eds.), Ceramics in Nuclear Waste Management, CONOF-790420, National Technical Information Service, Springfield, VA, 1979, p. 294.
[9] R.P. Turcotte, J.W. Wald, F.P. Roberts, J.M. Rusin, W. Lutze, Radiation damage in nuclear waste ceramics, J. Am. Ceram. Soc. 65 (1982) 589.

[10] M. Mathew, S. Tagaki, J. Res. Natl. Inst. Stand. Technol. 106 (6) (2001) 1035–1044.
[11] M. Wei, J.H. Evans, T. Bostrom, L. Grondhal, J. Mater. Sci.: Mater. Med. 14 (2003) 311–320.
[12] P. Trocellier, Ann. Chim. Sci. Mater. 25 (2000) 321–337.
[13] E. Fleet, Y. Pan, J. Solid State Chem. 112 (1994) 78.
[14] R. Venkata Krishnan, K. Nagarajan, Thermochim. Acta 440 (2006) 141.
[15] JCPDS-International Centre for Diffraction Data, PDF2 database, 1999. PDF-ID number -731728.
[16] JCPDS-International Centre for Diffraction Data, PDF2 database, 1999. PDF-ID number -830973.
[17] K. Sudarsanan, R.A. Young, Acta Crystallogr. B 30 (1974) 1381.
[18] R.D. Shannon, Acta Crystallogr. A 32 (1976) 751.
[19] D.D. Wagman, W.H. Evans, V.B. Parker, I. Halow, S.M. Bailey, R.H. Schumm, Selected Values of Chemical Thermodynamic Properties, National Bureau of Standards, Technical Note 270-3/7, Washington, 1968–73.
[20] O. Kubaschewski, C.B. Alcock, Metallurgical Thermochemistry (International Series on Materials Science and Technology, vol. 24), 5th edition, Pergamon Press Inc., Maxwell House, Fairview Park, Elmsford, Newyork, USA, 1979.